Chemical Physics Letters 502 (2011) 1–13

Contents lists available at ScienceDirect

Chemical Physics Letters

journal homepage: www.elsevier.com/locate/cplett

FRONTIERS ARTICLE

Applications and validations of the Minnesota density functionals

Yan Zhao [a], Donald G. Truhlar [b,*]

[a] Commercial Print Engine Lab, HP Labs, Hewlett-Packard Co., 1501 Page Mill Road, Palo Alto, CA 94304, USA
[b] Department of Chemistry and Supercomputing Institute, University of Minnesota, Minneapolis, MN 55455, USA

ARTICLE INFO

Article history:
Available online 19 November 2010

ABSTRACT

We discuss and review selected recent applications and validations of the Minnesota density functionals, especially the M06 family, emphasizing nanochemistry, organic, inorganic, and biological chemistry, and catalysis and highlighting the broad accuracy of these functionals as compared to previous popular functionals for thermochemistry, kinetics, and noncovalent interactions.

1. Introduction

Since 1993, density functional theory (DFT) in the formulation of Kohn and Sham [1], generalized to spin-polarized ground states by von Barth and Hedin [2], has become one of the most robust and popular quantum mechanical methods in computational chemistry and solid-state physics. Although Kohn–Sham DFT, including its generalization to spin-polarized systems (which includes all open-shell ground states) represents the accurate electron density as a single Salter determinant [1–3], it is an exact many-body quantum mechanical theory for the ground-electronic-state properties of a given system; however, it depends on an unknown (probably unknowable) universal exchange–correlation functional that can only be approximated. Finding better approximations is the primary concern of many theorists.

Many approximate density functionals have been published in the literature [4,5], and they can be classified as local or nonlocal. In order of increasing complexity and potential accuracy, the three popular types of functionals that we classify as local are the local spin density approximation (LSDA), which depends on the spin-labeled electron densities [1], generalized gradient approximations (GGAs) [6–11], which also depend on the reduced gradients (with respect to nuclear coordinates) of these densities (a reduced density gradient is a dimensionless quantity in which the spin-component density ρ_α is divided by $\rho_\alpha^{4/3}$), and meta-GGAs [12–16], which also depend on the spin-labeled noninteracting kinetic energy densities at a given point in space. Nonlocal functionals also involve an integral over all space. Nonlocal functionals include hybrid GGAs [17], hybrid meta-GGAs [12], doubly hybrid functionals [18,19], a functional designed to incorporate long-range dispersion interactions [20], and the random phase approximation [21].

Hybrid functionals include Hartree–Fock [HF] exchange operators, involving occupied orbitals, and doubly hybrid functionals also include nonlocal correlation terms involving unoccupied orbitals. Hybrid and doubly hybrid functionals have better performance for general-purpose applications in chemistry than do local functionals. B3LYP [7,8,17,22] is a hybrid GGA that was largely responsible for the early popularity of DFT in chemistry, and it is the most popular functional in chemistry [23]. Hybrid meta-GGAs [12,14,16,24–31] in which the energy depends on the occupied orbitals not only through the HF exchange terms (as in hybrid-GGAs) but also through the noninteracting spin-component kinetic energy densities [32–35] (as in meta-GGAs) have been shown to be capable of even better performance than hybrid GGAs [16,24,26–31].

We have developed several approximate functionals [11,14,18,26,27,29–31,36–44], culminating in the Minnesota 2005 functionals, M05 [29] and M05-2X [30], the Minnesota 2006 functionals, M06 [31], M06-L [14], M06-2X [14], and M06-HF [43], and the Minnesota 2008 functionals, M08-HX [44] and M08-SO [44]. In a recent review [16], we summarized some of our validations of the recently developed M06 family of functionals for broad areas in chemistry. The present article reviews selected recent applications and validations of the Minnesota functionals, with most of the focus on M06-L, M06, and M06-2X. M05 and M05-2X may be considered as earlier versions of M06 and M06-2X, respectively, and M08-HX and M08-SO may be considered as improved versions of M06-2X.

The present article will discuss some of the recent tests and successful applications, both for databases and for other problems. This review includes, among other topics, carbon nanochemistry, inorganic, organic, organometallic, and biological chemistry, electronically excited states, kinetics, and noncovalent interactions. The most significant new calculations reported here are in Section 10.

2. Theory

DFT is an exact theory of electronic structure. It provides an alternative to wave function theory (WFT), which is a retronym

* Corresponding author. Fax: +1 612 626 9390.
E-mail addresses: yan.zhao3@hp.com (Y. Zhao), truhlar@umn.edu (D.G. Truhlar).

0009-2614/$ - see front matter © 2010 Published by Elsevier B.V.
doi:10.1016/j.cplett.2010.11.060

used by Kohn [45] to distinguish the form of Schrödinger quantum mechanics that was almost universally applied to electronic structure theory before the advent of DFT, at which point in time WFT was often just called quantum mechanics. DFT does not deal with wave functions for real systems, although we have already mentioned that the Kohn–Sham formulation of DFT, which is used for almost all, but not quite all (see, e.g., Huang and Carter [46] and references therein) applications in chemistry, does involve orbitals in a Slater determinant that is used to represent the electron density of a system with noninteracting electrons but with the same density as the real system. The Slater determinant is introduced primarily as a device to calculate an approximation to the kinetic energy of the electrons; this approximation may be called the noninteracting kinetic energy. The final orbitals are determined by a self-consistent-field calculation that involves solving the so called Kohn–Sham or generalized Kohn–Sham pseudoeigenvalue equations for the orbitals of the Slater determinant; that calculation includes the noninteracting kinetic energy, the interaction of the electrons with the nuclei and any external field that may be present, the classical Coulomb interaction of the electron density with itself (which incorrectly allows electrons to interact with themselves, since classical electromagnetic theory does not recognize the quantization of charge), and a potential arising from a functional derivative of the so called exchange–correlation energy functional. This energy functional must therefore include everything else: the self-interaction correction, electron exchange, electron correlation, and the interaction correction to the noninteracting kinetic energy.

The Hohenberg–Kohn theorem assures us that an exact functional exists, but it is unknown and probably unknowable. However, the history of DFT has involved understanding it better and better and finding increasingly more useful approximations to it, and improvements, although often unsystematic, have been more rapid than in WFT, which is sometimes called systematically improvable. The approximations to the true density functional are usually called density functionals; we sometimes call them density functional approximations (DFAs).

Although the DFAs must also account for interacting kinetic energy, they are usually divided into two components, one called exchange and one called correlation. The partition, however, is different than the one used in WFT; in particular the exchange functional includes nondynamical correlation as well as exchange (note that exact exchange, because it is a result of antisymmetrization, would completely eliminate self-interaction), and the correlation functional includes only dynamical correlation. Systems for which a good zero-order wave function must contain nondynamical correlation are called multireference systems; this includes ozone and many open-shell bonding situations in transition metal chemistry. Nondynamical correlation, also called static correlation or near-degeneracy correlation [47], is the most difficult aspect of electronic structure theory, and essentially all DFAs still require improvement to reliably treat systems with high multireference character. One of the key advantages of DFT is that most DFAs automatically contain some static correlation ('for free'); one of the key disadvantages of DFT is that this static correlation is quirky and hard to control. (In WFT the treatment of static correlation is straightforward, in principle, by configuration interaction methods, but the cost of systematic methods very rapidly gets out of hand as system size increases, and the limit of practicality is already reached at ~16 statically correlated electrons.)

Let us return to the issue, mentioned in the Introduction, of what is a DFA a functional of. A key issue is that the most accurate DFAs depend on the Kohn–Sham orbitals, which are themselves functionals of the electron density. The first density functionals depended only on the total electron density, which may be computed from the occupied Kohn–Sham orbitals. This was quickly generalized to allow dependence on spin-up and spin-down electron densities and their local gradients. Stopping at this point yields what is called a generalized gradient approximation (GGA). Adding dependence on the local noninteracting kinetic energy densities for spin-up and spin-down electrons (τ_α and τ_β, or, for short, τ) yields what is known as a meta-GGA, which is still local (sometimes called semilocal). Adding nonlocal dependence on the orbitals by means of the Hartree–Fock exchange operator then yields what is called a hybrid meta-GGA. One can also add dependence on unoccupied orbitals [18,37] (see also [48] and references therein), but in the functionals emphasized here, we attempted to see how well one can do without using unoccupied orbitals, which raise the cost. Therefore a detailed discussion of the unoccupied-orbital functionals is beyond the scope of the present article. Range-separated functionals are very promising [49–53], but are also not covered in detail.

The key to improved performance of DFAs, at least in the functionals presented here, is the choice of functional form and the parametrization against a broad set of experimental (or high-quality theoretical) data. Including a large number of parameters will only produce good results if the functional form is well chosen. We experimented with a variety of functional forms chosen both to allow satisfaction of key constraints and to build in the correct physics. We found that kinetic energy densities (τ_α and τ_β) are very powerful in improving the functional form and our most accurate general-purpose functionals also include a finite percentage of Hartree–Fock exchange. We use Hartree–Fock exchange and τ to tame self-interaction, we use GGA exchange and τ to try to control nondynamical correlation in DFT exchange, and with improved exchange, we can improve correlation, whose deficiencies can otherwise be hidden among errors in the larger exchange terms. Some indication that we were on the right track was already provided by our successful BB1K [26], MPWB1K [27], MPW1B95 [27] functionals, which showed improved performance with only one new parameter each and our PW6B95 and PWB6K functionals [40] which showed encouraging success with six parameters each. We later found we could increase the number of parameters to 20, 30, or even 50 in a stable way, and this can provide improved performance. We found that even our functionals with a large number of parameters have a history of working well on kinds of chemical problems not represented in the training set, and this is one justification of their physicality. We note that counting parameters is an ambiguous and not very meaningful exercise; for example, some workers do not count parameters fit to the uniform electron gas or to theoretical data, parameters fit to exact or approximate constraints, or parameters inherited from previous functionals, and almost nobody counts choosing between which constraints to satisfy or not to satisfy (which is usually done on an empirical basis and which affects the performance of all GGAs and hybrid GGAs) as a parameter. In the final analysis, we value new density functional approximations based on their ability to successfully predict new chemistry and physics or explain existing chemistry and physics.

Our organized testing sets consist of 854 data in 54 databases including main group and transition metals and including both standard thermochemical data and data sensitive to medium-range correlation energy, like barrier heights and noncovalent interactions. A fraction of this data is also used for training. In addition, we and others have also tested our DFAs on many problems quite different from those in our databases. As a result of their design, and as result of these tests, we can make the following recommendations for the members of the M06 family, which have complementary strengths. We recommend M06 as a general-purpose functional applicable to both the main group and transition metals, but M06-2X is recommended if the problem has no multireference character and no transition metals. M06-L is very

fast for large systems, and is an excellent choice for transition metals and for calculating geometries for any system. M06-HF is recommended for problems that are extremely sensitive to self-interaction, such as long-range charge transfer excitations. All four functionals have good performance for van der Waals interactions, but M06-2X is the best for such interactions, especially for the very difficult case of π–π stacking. M05 and M05-2X are early versions of M05 and M05-2X, and M08-HX and M08-SO are improved versions of M06-2X.

At various places in the discussion that follows we compare to results of WFT methods; in these comparisons we use the following acronyms for WFT methods: HF, Hartree–Fock; MP2, second-order perturbation theory; SCS-MP2, spin-component-scaled MP2; CASPT2, multi-configuration MP2; MP3, third-order perturbation theory; G3 and G3B3, Gaussian-3 multilevel methods; QCISD, quadratic configuration interaction with single and double excitations; QCISD(T), QCISD with a quasiperturbative treatment of connected triple excitations; CCSD(T), like QCISD(T) except coupled cluster instead of QCI; df-LCCD(T0), density-fitting local coupled cluster theory with single, double, and local perturbative connected triple excitations. BCCD(T), coupled cluster method based on Brueckner orbitals with double excitations and a quasiperturbative treatment of connected triple excitations; ADC(2), second-order algebraic diagrammatic construction method; and W1 and W4, Weizmann-1 and Weizmann-4 multilevel methods. References for these methods are given in the articles cited.

In both DFT and WFT, basis sets are very important, but except in a few places where they are essential to the discussion, this review does not discuss basis sets.

3. Carbon and hydrocarbon nanochemistry

Nanochemistry is an active, recently emerged research area focusing on materials structured on a nanometer scale and their resulting chemistry. Experiments on nanomaterials are very challenging, and DFT studies on nanomaterials provide a useful complement to experimental investigations. Carbon and hydrocarbon nanostructures, including fullerenes and graphene sheets, are especially interesting.

In 2008, we employed M06-L and M06-2X to characterize the host–guest interactions in supramolecular complexes in a hydrocarbon nanoring [54] and concave-convex π–π interactions in buckyball nano-tweezers [55]. Both functionals have also been employed to calculate the structures and potential energy surface of coronene dimers [56], which are prototypical models for π–π interactions between graphene sheets but which have been too large for accurate WFT studies. Because of the importance of π–π stacking, Kishore et al. [57] used M06-L and M06-2X to calculate the binding energies in a zipper assembly of yellow *p*-oligophenyl naphthalenediimide (POP-NDI) donor–acceptor hybrids. Lim and Park [58] employed M06-2X, M06-HF, and M06-L to investigate noncovalent sidewall functionalization of carbon nanotubes, and their study shows that aromatic molecules have greater binding strength than saturated nonaromatic molecules due to the π···π stacking interactions.

Lee and McKee [59] carried out a theoretical study of endohedral hydrogen exchange reactions in high-pressure nano cookers (C_{60}, C_{70}, and C_{82}), and they found that M06-2X is in much better agreement with WFT results (MP2 and SCS-MP2) than is the popular B3LYP functional. M05-2X and M06-2X correctly account for the reduced repulsion between endohedral hydrogen molecules and enclosing C_{60}, C_{72}, and C_{82} fullerenes.

Osuna et al. [60] theoretically analyzed the Diels–Alder cycloaddition between cyclopentadiene and C_{60} for which experimental results on energy barriers and reaction energies are known, and they recommended the M06-2X functional for the high-level method in dual-level schemes for the study of the chemical reactivity of [6,6]-bonds in fullerenes and nanotubes. Based on these benchmarking results, Izquierdo et al. [61] employed the recommended methods to study regioselective intramolecular nucleophilic addition of alcohols to C_{60}, which provides one-step formation of a bicyclic-fused fullerene with an oxygen-containing five-member ring.

Vura-Weis et al. [62] used M06-2X to characterize the geometry and electron coupling in perylenediimide (PDI) stacks, which are promising candidates for organic thin film transistors (OTFTs) and organic photovoltaics (OPVs). They also employed M06-2X to screen 20 PDI derivatives by correlating stacking geometry with binding energy and electron coupling, and they identified the most promising candidates for incorporation into devices such as OTFTs and OPVs. They concluded that this 'strategy of side-by-side comparison of binding energy and electronic coupling may prove useful for other π-stacked OTFTs such as pentacene and poly (thiophene) derivatives.'

Peverati and Baldridge [63] used M06-2X and other functionals to study interactions in nanoscale polynuclear carbon-based complexes that have dominant dispersion-like interactions. The M06-2X functional provided consistently good agreement with respect to experiment.

Prakash et al. [64] used M05-2X to study sequential hydration in protonated carbonic acid–water clusters. They observed Eigen → Zundel → Eigen transitions in proton transfer from carbonic acid to water.

4. Organic chemistry

Evidence that modern functionals significantly exceed the performance of the popular B3LYP functional for organic chemistry has been presented by many research groups [65–76]. Some recent validations [77–82] have shown that M06-2X has much improved performance for main-group organic chemistry as compared to B3LYP. A key reason for this improved performance is the improved treatment of medium-range correlation energy, which includes overlap dispersion interactions, that is, dispersion-like attractive interactions at geometries where orbital overlap (and hence exchange repulsion) of the interacting subsystems cannot be neglected [82].

Garr et al. [83] applied M06-2X with a continuum solvation model to the 4 + 2 Diels–Alder cycloadditions of indole arynes and thioindole arynes to 2-substituted furans to study the unusual regioselectivity that sometimes leads to the more crowded product. The density functional calculations explained the results by showing that the 6,7-indolynes are highly polar structures and that the cycloadditions have substantial electrophilic substitution character such that the synchronicity of the reaction path and the preference for contrasteric products are sensitive to the electron-withdrawing or electron-donating character of the 2-substituent.

Sadowsky et al. [84] applied M06-L, B3LYP, and CASPT2 to [*n*]-cyclacenes ($n = 6–12$) to calculate strain energies and the degree of di- or poly-radical character inherent in the electronic structures. They found that the M06-L results are in better agreement with the more expensive and more difficult WFT calculations than are the results obtained with the popular B3LYP method.

M06-2X was used by Aginagalde et al. [85] to investigate the reaction between benzynes and imidazo[1,2-a] pyridines (pyrimidines) to form benzo[*a*]imidazo-[5,1,2-*cd*]indolizines, and 2,3,9c-triazocyclopenta[*j*,*k*]fluorenes has been studied computationally and experimentally. They found that these reactions take place via tandem $[\pi 8_s + \pi 2_s]$ and $[\sigma 2_s + \pi 6_s + \sigma 2_s]$ processes, with both synchronous and asynchronous reaction

paths being found (depending on the process), and the calculated results were consistent with the experimentally observed regioselectivity.

Bao et al. [86] employed M06-2X to investigate gated molecular basket systems, and they found that the molecular framework of gated baskets promotes the conformation interconversion of cyclohexane by more favorable noncovalent binding, thereby stabilizing the transition state.

Bertran et al. [87] carried out calculations for the structures and electronic properties of the optically active regioregular poly[(*R*)-3-(4-(4-ethyl-2-oxazolin-2-yl)phenyl)thiophene] and its model oligomer. They found that the M05-2X, M06-2X, and ωB97X-D [52] functionals lead to a change in the helical symmetry as compared to HF theory. HF calculations predict a helical turn with six repeating units, whereas the turn increases to seven repeating units per turn with the M05-2X, M06-2X, and ωB97X-D methods.

Wallevik et al. [88] studied the conformational properties of 1-silyl-1-silacyclohexane and found that M06-2X performs satisfactorily for the free energy difference of the axial and equatorial conformers, whereas B3LYP greatly overestimates the stability of the equatorial isomer. It is interesting that M06-2X agrees with experiment better than CCSD(T) or a doubly hybrid functional. Liu et al. [89] used M06 to explain the detonation sensitivity of silicon pentaerythritol tetranitrate (Si-PETN) explosive, and they showed that M06 is much more accurate than B3LYP for the prediction of bond dissociation energies of nitrile esters. In a recent feature article, Zhang et al. [90] reported that DFAs perform poorly for the enthalpy of the reaction:

$$CF_4 + SiCl_4 \rightarrow CCl_4 + SiF_4$$

We found, however, that using adequate polarization functions reduces the error of DFAs for the heat of reaction from ∼9–12 kcal/mol to ∼2–4 kcal/mol, and using the M08-SO density functional further reduces it to ∼1 kcal/mol [91].

Meyer and Kass [92] found that M06–2X, but not B3LYP, correctly indicated that the acidity order of the carbons in 2-adamantanone is β (axial) > α > β (equatorial).

Lignin is an underused component of biomass and a potential source of clean fuels and chemicals. Beste and Buchanan [93] employed M06-2X to calculated bond dissociation enthalpies for lignin model compounds. They found that the oxygen–carbon bond dissociation enthalpy is substantially lowered by oxygen substituents situated at the phenyl ring adjacent to the ether oxygen. In later work [94] they used M06-2X to study hydrogen abstraction reactions.

Recently we have reported a comparative assessment study for the energetics of the anti-E2, syn-E2, and S_N2 reactions of F^- and Cl^- with CH_3CH_2F and CH_3CH_2Cl, and we found that M06-2X give the best performance [95].

Wiitala et al. [96] employed M06 to investigate the mechanisms for a thermal decarbonylation of penam β-lactams. The calculated free energy of activation differences are in accord with experimental observations and support their proposed mechanism.

Powoski et al. [97] studied the conformers of butyryl chloride by chirped pulse Fourier transform microwave spectroscopy. They showed that M06-2X calculations predict a structure that agrees well with the experimental determination of the rotational constants. Rayne and Forest [97a] examined 562 isomerization enthalpies for pure and nitrogen-, oxygen-, sulfur-, and halogen-substituted hydrocarbons. They found that M06-2X offers nearly equivalent accuracy to 'higher level and much more expensive' WFT methods 'across all hydrocarbon classes.'

5. Excited states

Although DFT is a ground-state theory, approximations to excited states can be found by applying a time-dependent electric field. Excited states then show up as poles of the generalized polarizability. This is called time-dependent DFT (TD-DFT). Just as DFT has become the method of choice for ground-state structures, energetics, and properties of complex systems, TD-DFT has become the method of choice for excited states for all but the smallest systems. Thus there is great interest in learning which functionals are successful for calculating excited electronic states.

Our original tests of the Minnesota functionals for spectroscopy were very encouraging, especially for M06-2X, which gave excellent results for both valence and Rydberg excitations [31]. A subsequent study found the M08-HX gave the best results (out of 13 functionals tested) for multiplicity-changing excitations of molecules [43]. Jacquemin et al. [98] tested 29 density functionals, including M05, against a much larger database of singlet-to-singlet valence excitation energies, and together we [99] extended that study to M05-2X and the M06 family. Now we found that M06 has better general performance for electronically excited states than M06-2X, which in retrospect may be unsurprising since all electronically excited states are open-shell systems, and many of them have multireference character. In fact, for the 190 valence excitations in the set, PBE0 [100,101], B98 [102], B3LYP, M06, and M05 were the five best performing functionals with mean absolute deviations from the best estimates in the range 0.19–0.25 eV. However, none of these functionals has a mean absolute deviation from the best estimates for Rydberg states that is less than 0.86 eV. The third class of excitations is charge transfer states, which we consider next.

The accurate prediction of long-range charge transfer excited states is a long-standing problem [103,104] of DFT, and M06-HF [43] was designed to handle this type of excitation. Recently our group [105] showed that the M06-2X and M08-HX density functionals perform better than the range-separated CAM-B3LYP functional [106] for charge transfer excitations with intermediate spatial overlap. Moreover, M06-2X and M08-HX have better performance for bond energies, noncovalent interactions, and chemical reaction barrier heights for representative systems. Thus M06-2X and M08-HX should be preferred for studies requiring the exploration of potential energy surfaces as well as electronic excitation energies, provided that those excitations with very long-range charge transfer are excluded.

Marenich et al. [107] carried out a systematic study to sort out the relative contributions of electrostatic polarization, dispersion, and hydrogen bonding to solvatochromic shifts on vertical electronic excitation energies. Their TDDFT calculations employing corrected linear response theory [108] to include continuum solvation with the M06 functional for 23 solvents reveal a dispersion contribution to the red of 261–356 cm^{-1} and a hydrogen-bonding contribution to the blue of up to 289 cm^{-1}. Unfortunately these nonelectrostatic contributions have often been neglected in applications in the recent literature.

Santoro et al. [109] found that M05-2X provides a picture close to that of CASPT2 for the lowest excited states of π-stacked cytosine dimer, whereas other DFAs examined underestimate the binding energy.

Aquino et al. [110] performed a benchmark study of electronic singlet excitations of stacked adenine–thymine (AT) and guanine–cytosine (GC) with the ADC(2) method. They assessed the performance of the M06-2X, M06-HF, B3LYP, and PBE0 methods. The M06-2X functional provides a relatively good reproduction of the ADC(2) results. It avoids the serious over-stabilization and overcrowding of the spectrum found with the B3LYP method. On the

other hand, M06-HF destabilizes the charge transfer state too strongly. M06-2X calculations in solution (heptane, isoquinoline, and water) using the polarizable continuum model (PCM) and the linear response formalism [111] show a stabilization of the charge transfer state and an increase in charge transfer character with increasing polarity of the solvent.

Świderek and Paneth [112] have studied five iridium Ir(III) complexes using the B3P86 [113], B3LYP, M05, M06, M05-2X, and M06-2X functionals. Their results indicate that the M05-2X functional gives excellent results for reliable prediction of emission properties with the exception of the $(bsn)_2Ir(acac)$ complex, and the discrepancy in that case is due to the presence of the sulfur atom.

Patel and Masunov [114,115] employed TD-DFT with the linear response formalism to include continuum solvation to calculate absorption spectra of 29 diarylethene derivatives. They found that M05-2X gave the most accurate predictions of bond length alternation (see also [116]), and M05 at M05-2X geometries gave the best agreement with experiment for spectral data of both open and closed isomers.

Kim et al. [117] performed DFT and multiconfiguration WFT calculations of geometries, vibrational frequencies, and vertical excitation energies (T_v) for the CF_2ICF_2I and $CF_2ICF_2^-$ molecules. They found that the M05-2X functional performs well for the prediction of molecular geometries and electronic excitation energies as compared to CASPT2, but it overestimates the vibrational frequencies. We have recently developed a universal scale factor strategy [118] to correct systematic errors in vibrational frequencies. The electronic excitation energies of CF_2ICF_2I were calculated by the linear response method with continuum solvation in methanol; it was found that B3LYP underestimates them, whereas M05-2X is in best agreement with experiment [117].

Intensities for vibrational Raman spectroscopy have also been studied [119]. Such intensities depend on derivatives of molecular polarizabilities with respect to nuclear coordinates. Although the authors expected Hartree–Fock exchange to be essential for accurate calculations of Raman intensities, they found good results even with M06-L, which has none. However, out of ten functionals tested, M06-HF gave the most accurate Raman intensities.

6. Inorganic chemistry

In this section, we review recent validations and applications of the Minnesota functionals in inorganic chemistry.

Meyer and Kass [120] calculated gas-phase acidities, bond dissociation energies, and heats of formation of $HClO_x$, $x = 1–4$ with B3LYP, M06, M06-2X, and two WFT methods: G3 and G3B3. By comparing to the experimental results, they found that all of the methods 'do a reasonable job for the first three thermodynamic quantities, but only M06 does a satisfactory job for the heats of formation, and its performance is similar to the highly accurate but extremely time-intensive W4 method.'

Plumley and Evanseck [121] have benchmarked our functionals in modeling the binding enthalpies of substituted B–N coordinate covalent bonds. The mean unsigned error (MUE) from experimental binding enthalpies for M06-2X and M05-2X is 0.3 and 1.6 kcal/mol, respectively. M06-2X yields a lower MUE than more expensive WFT methods (MP2, 1.9 kcal/mol; QCISD, 2.3 kcal/mol; QCISD(T), 0.4 kcal/mol). They showed that M06-2X provides a balanced account of the short- and medium-range exchange–correlation energies necessary to accurately describe the binding enthalpy of coordinate covalent bonds in sterically congested molecular systems. More recently, Janesko [122] compared the performance of the different functionals for the prediction of dative bonding in substituted boranes. His results also support Plumley and Evanseck's conclusion that the Minnesota functionals are very accurate for dative bonding.

Dias et al. [123] employed M06 to investigate the electronic and spatial effects of different phosphorus ligands on the selectivity of the olefin (propene and styrene) insertion reaction into the RhH bond of the complexes $HRh(PR_3)(CO)_2$(olefin). They found that M06 results are in good agreement with the experimental findings.

Austin et al. benchmarked several functionals for actinyl complexes [124] and they found that the M06 functional is competitive with high-level CCSD(T) methods in the study of the water exchange mechanism of the $[UO_2(OH_2)_5]^{2+}$ ion and of the redox potential of the aqua complexes of $[AnO_2]^{2+}$ (An = U, Np, and Pu). Oncák et al. [125] found the M06 family to be slightly superior to B3LYP for the structure and energetics of uranium species formed upon hydrolysis of uranyl nitrate. In recent work (Averkiev, Mantina, Valero, Infante, Kovacs, Truhlar, and Gagliardi, unpublished), we found that the MPW3LYP, B3LYP, M05, and M06 functionals give similar mean unsigned errors to CASPT2, CCSD, and CCSD(T) calculations for actinoid–oxygen bond energies and for ionization potentials of actinoid oxides and their cations.

7. Organometallic complexes and catalysis

The computer-aided design of new catalysts is challenging, and the emergence of more accurate density functionals and the increase in computer power have opened up new opportunities for theoretical and computational understanding of the structures and mechanisms in new catalytic systems and for guiding the design of more efficient catalysts for various important problems such as olefin metathesis and cross coupling, organic oxidation, nitrogen fixation, water oxidation, and hydrocarbon functionalization. Both heterogeneous and homogeneous catalysis are important, here we discuss heterogeneous catalysis first.

In 2008, we developed a benchmark database for interactions in zeolite model complexes based on CCSD(T) calculations, and we tested 41 density functionals against the new database [126]. We also tested 10 functionals against the binding energies of four complexes (two noncovalent and two covalent) representing possible modes of the adsorption of isobutene on a large 16T zeolite model cluster (an '*n*T' cluster is one with *n* tetrahedral centers), and we found that M05-2X and M06-2X are the best performers for the binding energies in a model 16T zeolite cluster, followed by M06-L and M06, and these four functionals give a smaller MUE than the MP2 method. The popular B3LYP functional performs poorly with an MUE of 16.6 kcal/mol. These results show that M06-L, M06, M05-2X, and M06-2X are very promising quantum mechanical methods for the QM part of QM/MM simulations of zeolite. This conclusion has recently been confirmed by Maihom et al. [127]. They investigated the mechanisms of ethene methylation with methanol and dimethyl ether in a 128T cluster of ZSM-5 zeolite using B3LYP and M06-2X combined with molecular mechanics, in particular with the universal force field (UFF) parameters, with the zeolitic Madelung potential generated by the surface charge representation of the electrostatic embedding potential (SCREEP) method [128]. Their calculations show that the energies for the adsorption of methanol and dimethyl ether on H-ZSM-5 from M06-2X:UFF + SCREEP calculations are in good agreement with the experimental data.

Boekfa et al. [129] employed four dual-scale methods, namely MP2:M06-2X, MP2:B3LYP, MP2:HF, and MP2:UFF, to investigate the confinement effect on the adsorption and reaction mechanism of unsaturated aliphatic, aromatic, and heterocyclic compounds on the ZSM-5 zeolite. They found the best agreement with experiments for the energies of adsorption of ethene, benzene,

ethylbenzene, and pyridine when M06-2X was used to describe the large-scale framework subsystem.

Kumsapaya et al. employed the M06-L:UFF method to investigate the isomerization of 1,5- to 2,6-dimethylnaphthalene over acidic β zeolite [130]. The results in their study show the excellent performance of a combination of the M06-L functional with the confinement effect represented by the universal force field for investigating the transformations of aromatic species in the zeolite systems.

Maihom et al. [131] investigated the effects of the zeolite framework on the mechanism of *n*-hexane monomolecular cracking with M06-2X calculations. The calculated adsorption energies of hexane in the H-FAU and H-ZSM-5 zeolites are in good agreement with experiments. Their results indicate that confinement effects on different types of zeolites can be well represented by the M06-2X functional.

Labat et al. [132] studied the performance of nine density functionals for equilibrium geometries and binding energies of water interacting with clusters modeling the silcate-1 zeolite and found the best performance for M05-2X and B97-D [133], where '-D' denotes the inclusion of an empirical molecular mechanics term to account for long-range dispersion.

Now we turn to homogeneous catalysis. Yang et al. [134] recently tested 34 density functionals against two representative databases for diverse bond energies and barrier heights in catalysis. The bond energy database includes metal–metal bonds, metal–ligand bonds, alkyl bond dissociation energies, and atomization energies of small main group molecules. The RPBE [135] and revPBE [136] functionals, widely used for catalysis, do improve the performance of PBE against the two diverse databases, but give worse results than B3LYP. Overall, M05, M06, and M06-L give the best performance for the two diverse databases, which suggests that they deserve more attention for applications to catalysis.

Tsipis et al. [137] reported that some popular functionals fail to predict the trend of the phosphine binding energies between the first- and second-generation Grubbs' ruthenium precatalysts for olefin metathesis. Experiments show that the phosphine dissociation in $(PCy_3)_2Cl_2Ru=CHPh$ is faster than in $(H_2IMes)(PCy_3)Cl_2Ru=CHPh$ [138,139], where Cy, Ph, and IMes are cyclohexyl, phenyl, and 1,3-dimesitylimidazol-2-ylidine. We have shown [16,140] that the M06 suite of functionals predict the right trend of bond dissociation energies (BDEs) whereas B3LYP and other popular functionals predict the wrong trend for the BDE difference. After we submitted our paper to *Org. Lett.*, one of the referees raised an issue about the absolute gas-phase values of the M06-L calculated BDE, which are about 10 kcal/mol greater than those inferred from the condensed-phase experiments of Sanford et al. [138]. We argued that it was important to predict the correct trends even if the absolute values were less accurate, and anyway the 10 kcal/mol difference could have been due to complicated condensed-phase effects; so our work was accepted and published in a timely fashion. One year later, Torker et al. [141] performed a gas-phase measurement of the BDEs of the Grubbs catalysts, and the gas-phase experimental BDEs agree very well with our gas-phase M06-L calculations. It is encouraging that our M06-L prediction was published before the experimental validation. In 2008, we employed a high-level method, CCSD(T), to create a benchmark database for energetics in a model Grubbs II metathesis catalysis [142]. We also used this database to test 39 density functionals, and we confirmed that M06-L and M06 perform very well, and B3LYP and other functionals containing the LYP correlation functional perform poorly. Sliwa and Handzlik [143] have done a similar benchmark calculations for Grubbs I metathesis catalysis, and they concluded that the M06 method gives the best performance.

Pandian et al. [144] employed the M06, M06-L, and B3LYP functionals to predict the reaction path energetics of ring formation via diene ring closing metathesis with Grubbs Ru-based catalysts. They benchmarked the three functionals against a high-level WFT energy of reaction (obtained by CCSD(T)) for addition of ethylene to a ruthenium methylidene model compound to form a metallacyclobutane, and they found that M06 and M06-L agree with the high-level result within 1.6 kcal/mol, whereas B3LYP differs by 10 kcal/mol.

Benitez et al. [145] employed B3LYP and M06 to investigate a long-standing controversy in the mechanism of Grubbs Ru-based catalysis. They show conclusively that the intermediate complex in the olefin metathesis mechanism of Grubbs second-generation catalyst is bottom-bound with the chlorides remaining *trans* throughout the reaction. More recently they [146] employed M06 to settle a long-standing disagreement of DFT with experiment for the phosphine dissociation in Grubbs metathesis catalyst. By comparing to recent solution NMR data, they found that M06 leads to more accurate predictions for the stability of conformers than B3LYP.

Stewart et al. [147] performed an assessment of B3LYP and M06 for the conformations of Ru-based catalyst with the N-heterocyclic carbene and *N*-tolyl ligands. They found that B3LYP provides geometries that match X-ray crystal structural data more closely, but it leads to slightly less accuracy than M06 due to the underestimation of the attractive noncovalent interactions.

Sieffert and Bühl [148] calculated the BDE of a triphenylphosphine ligand in $Ru(CO)Cl(PPh_3)_3(CH=CHPh)$ with 'popular' (BP86 [8,149] and B3LYP), dispersion-corrected (B3LYP-D [133] and B97-D [133]), and the M06-class functionals, and they found that 'B97-D and the M06 series of functionals best reproduce the experimental binding enthalpy value of Sponsler et al.' In later work [150], they found that M06-L is better suited than B97-D for describing the enthalpy of activation for H_2 dissociation from a ruthenium triphenylphosphine complex. Minenkov et al. [151] have tested density functionals for predicting metal-phosphine bond strengths in a series of phosphine complexes of Cr, Ni, Mo, and Ru. They also found that DFT-D and M06 functionals perform much better than popular density functionals.

Because of its good performance for weak bonding interactions, Huang et al. [152] selected the M05-2X density functional to study the first metal-free N-heterocyclic carbene-catalyzed conversion of CO_2 to CH_3OH. The calculations explain the experimental finding that the phenylsilane reaction is more efficient than the diphenylsilane reaction.

Bozoglian et al. [153] employed M06-L to calculate the relative energetics of alternative reaction pathways and potential intermediates associated with the oxygen–oxygen bond formation promoted by a Ru-Hbpp water oxidation catalyst. In particular, they characterized stationary points along different reaction paths at the M06-L level and then assessed the reliability of various aspects of the DFT calculations by comparing to CASPT2. They found that M06-L and CASPT2 make very similar predictions for state energy splittings in individual complexes.

Fedorov et al. [154] synthesized a gold carbene complex, and they also measured the PPh_3 dissociation energy from collision-induced dissociation (CID) energy-resolved cross section measurements under near single-collision conditions and compared the experimental value with M06-L and B3LYP calculated results. The CID experiments yielded a bond dissociation energy of 51.7 ± 3.3 kcal/mol at room temperature. By using M06-L zero-point energy and thermal corrections, we obtain an 'experimental' value of the equilibrium bond dissociation energy, D_e, from their D_{298}; the result is $D_e = 58.5 \pm 3.3$ kcal/mol. Their M06-L calculations give a D_e of 58.8 kcal/mol, which is in excellent agreement with the value derived from the CID experiments, whereas B3LYP

underestimates D_e by about 28 kcal/mol. In further work, Fedorov et al. [155] performed an experimental and theoretical study of a gold(I) aminonitrene complex in the gas-phase. They found that the M06 family of functionals gives the best performance for reproducing the thermochemistry inferred from the threshold collision-induced dissociation experiments.

Benitez et al. [156] employed M06 to analyze a bonding model for gold carbene complexes, and they concluded that the reactivity in gold(I)-coordinated carbenes is best accounted for by a continuum ranging from a metal-stabilized singlet carbene to a metal-coordinated carbocation. The position of a given gold species on this continuum is largely determined by the carbene substituents and the ancillary ligand. In subsequent work, Benitez et al. [157] used M06 to study the impact of steric and electronic properties of ligands on gold(I)-catalyzed cycloaddition reactions, and they concluded that the impact of the gold catalyst on migratory aptitude is a consequence of the relative strength of the dπ to pπ interaction in the Au–C bond. Importantly, these results suggest that the sterics of the ligand can dramatically impact Au–C bonding.

Nyhlén and Privalov [158] performed calculations for the $B(C_6F_5)_3$-catalyzed hydrogenation of unsaturated carbon–heteroatom bonds with a number of density functionals, and they found that there is substantial difference between results obtained with different functionals even for structurally simple species. Of nine functionals tested, M06-2X gave the best agreement with high-level WFT for the energy of addition of H_2 to carbonyls.

Catalysis by Pd compounds has a long history [159–162], and Pd catalysts are widely used in the pharmaceutical industry. Sakaki and coworkers [163] showed that popular DFAs systematically underestimate the binding energies of alkenes and polyenes to Pd and Pt complexes, and the error becomes very large when the size of the conjugated system is increased. In collaboration with Averkiev, we have performed a BCCD(T) benchmark study [164] of the binding energies of $Pd(PH_3)_2$ and $Pt(PH_3)_2$ complexes with ethene and conjugated C_nH_{n+2} systems ($n = 4$, 6, 8, and 10). We found that the Minnesota DFAs (M06 and M06-L) agree well with the best estimates. The mean unsigned error in absolute and relative binding energies of the alkene ligands to $Pd(PH_3)_2$ is 2.5 kcal/mol for the ωB97 [52] and M06 density functionals and 2.9 kcal/mol for the M06-L functional. Adding molecular mechanics dispersion yields even smaller mean unsigned errors: 1.3 kcal/mol for the M06-D [165] functional, 1.5 kcal/mol for M06-L-D [165], and 1.8 kcal/mol for B97-D [133] and ωB97X-D [166]. The new functionals also lead to improved accuracy for the analogous Pt complexes. These results show that recently developed density functionals may be very useful for studying catalytic systems involving Pd d^{10} centers and alkenes.

Mutter and Platts [167] employed a series of ab initio methods to determine the C–H···π and π···π stacking interactions of aromatic rings coordinated to transition-metal centers. They also used the benchmark data to assess the performance of some lower-cost methods including DFT. They found that one version of the spin-component scaled MP2 method (a WFT method) performed well in all cases. BHandH (a functional similar to that proposed by Becke [168]) and M06-2X perform better than M05-2X.

Huang and Lee [169] employed B3LYP, BMK, and M05-2X to study the CO adsorption on Pt nanoclusters. They found that BMK [28] and M05-2X give a better unbound description of CO $2\pi^*$ LUMO than the popular B3LYP functional.

Couzijn et al. [170] studied a phenylpalladium(II) N-heterocyclic carbene complex by using collision-induced dissociation threshold measurements to obtain quantitative gas-phase thermochemical data for reductive elimination and ligand dissociation. They also found that M06-L reproduces the experimental energetics well.

Metallinos et al. [171] performed a joint experimental and computational investigation of the asymmetric lithiation of boron trifluoride-activated aminoferrocenes. They found that M06-2X correctly predicts both the sense and extent of chiral induction.

Dutta et al. [172] employed M06 in combination with a continuum solvent model to investigate the first elementary steps of the reaction of mono(η^2-alkyne) half-sandwich catalysts containing $RuCl(Cp^*)$ and $RuCl(Cp^\wedge)$ fragments with alkynes, where Cp^* = η^5-C_5Me_5 and $Cp^\wedge$ = η^5-1-methoxy-2,4-tert-butyl-3-neopentyl-cyclopentadienyl. M06 combined with a continuum treatment of the solvent was able to rationalize and complement the experimental findings and was used to examine steric, substituent, and mechanistic effects.

Ruiz [173] employed the Minnesota functionals to calculated the small exchange coupling constants of dinuclear transition metals complexes involving V, Fe, and Cu. Their results indicate that the M05 and M06 functionals provide excellent coupling constants with similar accuracy to that of the best functionals previously tested. Exchange coupling constants in both organic and inorganic molecules had been studied earlier, and good results were obtained with both M06-L and M06 [174].

8. Kinetics

One of the ultimate goals of chemistry is to be able to understand and control chemical reaction systems. To realize this goal, one needs to determine the rates of chemical reactions. Computational thermochemical kinetics is the branch of theoretical chemistry that involves the prediction of the rate constants of chemical reactions by using information about the structures, energies, and vibrational frequencies (or vibrational free energies) of reactants and transition states, along with estimates of dynamical contributions (such as tunneling or recrossing) to the phenomenological free energy of activation. One key quantity for kinetics calculation is the barrier height of a given chemical reaction. We have developed benchmark databases of barrier heights – inferred from experiments and calculations – for diverse types of reactions [38,42,175], and these databases have been used in the assessment and development of new theoretical methods. Based on these databases, we also developed small sets of representative barrier heights as easier-to-use benchmarks for comparing and developing theoretical methods. The resulting DBH24 database [175] has been updated recently [42] by using more accurate theoretical data. The updated database is called DBH24/08; 348 model chemistries were assessed against DBH24/08 [42], and it was found that M08-SO gives a mean unsigned error of only 0.90 kcal/mol. In contrast, the much more expensive CCSD(T) method with the same cc-pVTZ basis set augmented with diffuse s and p functions on nonhydrogenic atoms has a mean unsigned error of 1.00 kcal/mol for the same database. The M05-2X, M06-2X, and M08-HX DFAs also perform well for barrier heights, and these four DFAs are well suited to be used as implicit potential energy surfaces (PESs) for direct dynamics [176–179] studies of reaction kinetics.

Kim et al. [180] described a general equilibrium-solvation-path formalism for studying liquid-phase reactions in terms of free energy surfaces, chemical potentials, pseudochemical potential energy surfaces, and solute–solvent coupling, with this coupling quantified in fixed-concentration free energies of solvation. They [180] used this formalism with the M06-2X density functional and the SM8 [181] continuum solvation model to explain how the α,β-elimination of the thioester methyl 3-mesyloxybutanothioate follows an $E1cB_{irrev}$ reaction path while the ester analog has a concerted but asynchronous E2 mechanism with an E1cB-like transition state.

The reaction of OH with H_2S provides a difficult challenge for theory because the barrier occurs in the early part of the reaction path where the noncovalent attraction and exchange repulsion must be treated in a consistent and balanced way. The M06-2X functional was successfully employed to explain the unusual temperature dependence of this atmospherically important reaction [182].

Hayama et al. [183] employed M06-2X to calculated the structures and kinetic isotope effects in the bowl–inversion process of pentaarylcorannulenes. They found that B3LYP gives large errors for the structures (especially for the bowl depth) and bowl–inversion barrier heights.

Zheng et al. [184] used M06 and M06-L to calculate the rate constant of the methyl–methyl radical association reaction by using variational transition-state theory with a variable reaction coordinate and a multifaceted dividing surface. They found that the best prediction of rate constants is based on the potential energies calculated by the M06-L density functional; these agree with experimental data quantitatively from 300 to 1000 K. More recently, Zheng and one of the authors [185] calculated the rate constants of three intramolecular hydrogen-transfer isomerization reactions, namely, 1–4 isomerization of the 1-pentyl radical and 1–4 and 1–5 isomerizations of the 1-hexyl radical, by using M06-SO and the doubly hybrid MCG3-MPW method. We [186] also employed M06-2X to calculate the rate constants of five isomerization reactions involving intramolecular hydrogen-transfer in butoxyl radicals.

Pabis et al. [187] employed M06-2X and B3LYP to calculate kinetic isotope effects on the S_N2 and E2 reactions between hypochlorite anion and ethyl chloride in water. They found that M06-2X gives more accurate structures and energetics than B3LYP.

M06-L was used by Kim et al. [188] to mechanistically analyze the base-catalyzed HF elimination from 4-fluoro-4-(4′-nitrophenyl)butane-2-one. The primary and secondary deuterium kinetic isotope effects and the leaving-group fluorine kinetic isotope effects were calculated, and mechanistic conclusions were drawn.

The question of steric effects versus solvation effects on S_N2 reactions is an old puzzle. Kim et al. [189] reported M06-2X calculations designed to analyze the influence of solvent effects and substituent effects on the S_N2 reactions of Cl^- with $CH_3CH(X)Cl$ and $(CH_3)_3CCH(X)Cl$ (for X = H and CN) in the gas phase and aqueous solution. They found that the smaller deceleration associated with aqueous solvation for X = H roughly balances the gas-phase acceleration predicted for X = CN so that the aqueous activation free energies for the substrates are predicted to be similar for these two substituents. Shortly afterwards, Chen et al. [190] studied the same systems with less reliable but complementary methods, and they came to similar conclusions.

9. Biological and medicinal chemistry

Quantum mechanical effects play very important roles in biological science for problems such as protein folding and nucleobase packing and stacking. The accurate description of quantum effects is also a key to understanding the mechanism of many enzyme-catalyzed reactions [191,192].

Suresh et al. [193] performed a systematic study of CH···π, OH···π, NH···π, and cation···π interactions using complexes of phenylalanine in its cationic, anionic, neutral, and zwitterionic forms with CH_4, H_2O, NH_3, and NH_4^+ at B3LYP, MP2, MPWB1 K, and M06-2X levels of theory. Their assessments show that both MPWB1K and M06-2X give better performance for noncovalent interactions than B3LYP.

Valdes [194] developed a benchmark energetic database (based on CCSD(T)) for five small peptides (WG, WGG, FGG, GGF, and GFA) containing the residues phenylalanyl (F), glycyl (G), tryptophyl (W) and alanyl (A), where F and W include aromatic groups. They assessed the performance of the MP2, SCS-MP2, MP3, TPSS-D [195], PBE-D [195], M06-2X, BH&H, TPSS [13], and B3LYP methods against this benchmark database (where '-D' again denotes addition of a molecular mechanics dispersion term). Among the tested DFT functionals, the M06-2X and TPSS-D functionals show the best performance.

Gu et al. [196] employed M06-2X to predict the structures and stacking interactions in uracil dimers and thymine dimers. Their study demonstrates that the M06-2X functional is able to predict stacked structures for the uracil and thymine dimers that are in better agreement than MP2 with CCSD(T) results.

In order to understand mechanisms of base selection by human single-strand selective monofunctional uracil-DNA glycosylase, Darwanto et al. [197] employed M06-2X to determine the solvation free energy of the various substituted uracil analogs.

Prolyl-leucyl-glycinamide (PLG) is an important tripeptide that modulates specific dopamine receptor subtypes of the D_2 receptor family within the vertebrate central nervous system. However, the exact PLG interaction site and structural feature on the D_2 receptor are unknown. Wood et al. [198] recently developed CCSD(T) benchmark data for the geometry of 4-methylthiazolidine, which is a small molecule that comprises key structural features present in the PLG-analog library geometry. They also assessed the accuracy of 12 density functionals, and they found the top five functionals for 4-methylthiazolidine were M05-2X, mPW1PW [199], B97-2 [200], M06-2X, and PBE0, with mean unsigned errors (MUEs) in bond length of 0.0017, 0.0020, 0.0023, 0.0025 and 0.0027 Å, respectively. The best local functional is M06-L with an MUE of 0.0030 Å.

Byler et al. [201] employed B3LYP and M06 to test the hypothesis that quinoline alkaloids may serve as intercalative topoisomerase inhibitors. They found that B3LYP completely fails to locate the π stacking minima between the known intercalators with adenine–thymine (AT) and cytosine–guanine (CG), whereas the M06 calculations indicated favorable π···π interactions between quinoline alkaloids and the CG base pair.

Ebrahimi et al. [202] theoretically analyzed the stacking interactions in the uracil:phenylalanine (U–Phe) and (U–Phe)···Na^+ complexes. They found that Na^+ can interact with different sites of a stacked U–Phe unit, and it influences the π···π interactions in U–Phe.

Cao and van Mourik [203] assessed the performance of M06-L for its ability to predict the correct structures of a Tyr–Gly conformer, for which MP2 and B3LYP are problematic. They found that M06-L yields 'excellent agreement with the reference profile computed by df-LCCSD(T0). Thus, M06-L manifests itself as a very promising method to investigate the potential energy surfaces of small peptides containing aromatic residues.' Toroz and van Mourik [204] investigated the structural preference of the gas-phase neutral glycine tripeptide by using a variety of theoretical methods. They used M05-2X and a functional including molecular mechanics terms to verify the structure and relative stabilities of the 20 most stable conformers. van Mourik et al. [205] used M05-2X and B3LYP to study the keto and enol tautomers of uracil and 5-bromouracil in nanodroplets of up to 100 water molecules.

Hargis et al. [206] examined noncovalent complexes of a tumorigenic benzo[*a*]pyrene (B*a*P) diol epoxide with the guanine–cytosine (GC) and adenine–thymine (AT) base pairs by using the M06-2X functional. M06-2X predicts five thermodynamically accessible complexes for AT with (+)-B*a*P DE-2 that are compatible with intact DNA, and two for GC···(+)-B*a*P DE-2. The computational results help elucidate the formation of adducts of (+)-B*a*P DE-2 with DNA.

Ortega-Castro et al. [207] reported a comprehensive theoretical DFT study (B3LYP and M06–2X) of the formation of Schiff bases of

pyridoxamine analogues with two different aldehydes. The reaction mechanism was found to involve two steps, namely: (1) formation of a carbinolamine and (2) dehydration of the carbinolamine to give the final imine. Also, the M06-2X calculations show that the carbinolamine dehydration is the rate-determining step of the process, which is consistent with available experimental evidence.

Rutledge and Wetmore [208] tested many low-cost methods against a database of 129 CCSD(T) interaction energies for stacked and T-shaped complexes of nucleotide bases and amino acids. They found that M06-2X and PBE-D [133] provide very promising performance. They tested 16 DFAs, including three Minnesota functionals, and they found the best performance for the Minnesota functionals (M06-2X, M06-L, and M05-2X). Of the remaining functionals, PBE-D was best but with a mean unsigned error 1.5–3 times larger than that of M06-2X.

Kang and Byun [209] tested density functionals for their ability to describe the conformational preference of the alanine dipeptide and the proline dipeptide. Their calculations show that the SMD continuum solvation model [210] reproduced experimental hydration free energies of the model compounds for backbone and side chains of peptides well. More recently, Kang et al. [211] explored the conformational preferences and prolyl *cis–trans* isomerizations of the (2S,4S)-4-methylproline (4S-MePro) and (2S,4R)-4-methylproline (4R-MePro) residues by using M06-2X in the gas phase and in water, where solvation free energies were again calculated using the implicit SMD model. Their calculated populations for the backbone structures of Ac-4S-MePro-NHMe and Ac-4R-MePro-NHMe in water are reasonably consistent with CD and NMR experiments.

Greenwood et al. [212] employed the M06-2X/aug-cc-pVTZ(-f) [PB-SCRF] method provide accurate energies for model tautomeric systems. They engineered a method for predicting lowest-energy tautomers by combining M06-2X calculations with linear free energy relations.

Kona and Tvaroska [213] tested seven density functionals (BLYP, B3LYP, MPW1PW91, MPW1K [36], MPWB1K, M05 and M05-2X) and two wave-function methods (HF and MP2) for the predictions of structures and energetics of the formation or dissociation of the glycosidic bond in sugar phosphates. Their assessment shows that MPW1K, M05, and M05-2X give the best performance for structures, whereas M05-2X, MPW1K, and MPB1K give the best performance for the prediction of the thermochemical kinetic parameters.

10. Noncovalent interactions

One of the important successes of the Minnesota functionals is their good performance for noncovalent interactions [14,16,31,44,54–56,77,126,140,214–217]. We attribute this to an improved description of medium-range correlation energy, where medium range is defined as longer range than typical covalent bond distances but shorter range than the long-range region where overlap of interacting subsystems can be neglected. Medium range includes the typical distance of interacting molecules in van der Waals complexes (where exchange repulsion is very significant) or the distance between geminal carbon atoms in organic chemistry. Our functionals do not describe long-range dispersion interactions, but they do describe medium-range dispersion-like interactions. In fact, at medium range, there is no exact distinction between dispersion and other types of electron correlation. The relative importance of the long-range dispersion depends on the problem. Noncovalent interactions were the key issue in several of the applications in Section 9, and here we discuss additional aspects.

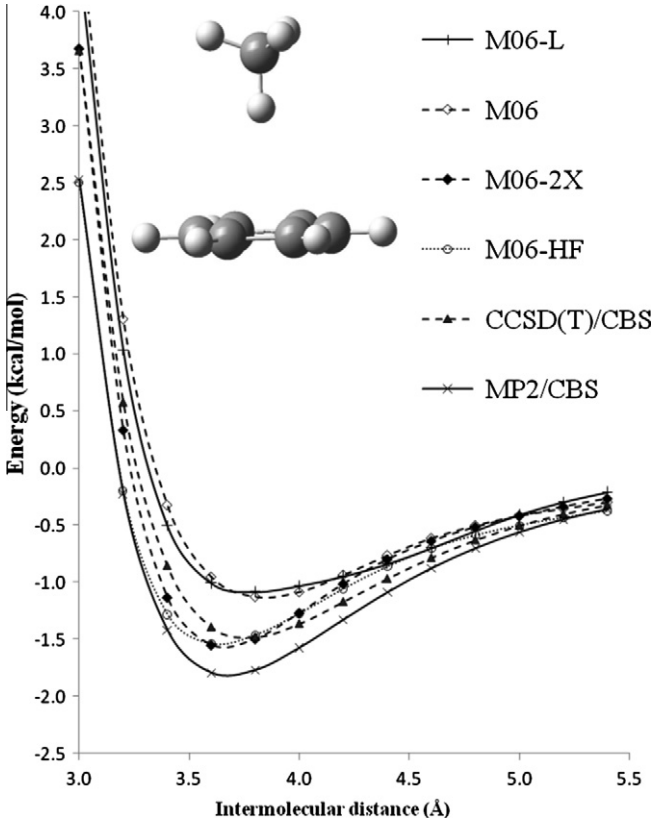

Figure 1. Binding energy curves for the C_6H_6–CH_4 complex with the 6-311+G(2df, 2p) basis set. The intermolecular distance is defined as the distance between the carbon atom in CH_4 and the C_6H_6 plane. The CCSD/CBS and MP2/CBS results (where CBS denotes the limit of a complete one-electron basis set) are taken from Shibasaki et al. [242].

Some recent papers [218,219] stated that our functionals describe noncovalent interactions by the exchange functional, but this is not correct. In order to better understand the physical origin of the noncovalent interactions, we compared the intermolecular potentials of the C_6H_6–CH_4 complexes. Figure 1 presents the full potential curves, whereas Figure 2 is for the exchange only calculations, and Figure 3 is for the correlation contributions. Figure 2 clearly shows that the exchange-only potential curves of the M06 family functionals are repulsive (even more repulsive than the HF calculations). Figure 3 tells us that the good performance of M06-class functionals for describing the medium-range part of noncovalent interaction is because M06 functionals have better correlation functionals, which give the attractive contribution to the noncovalent interactions.

Dahlke et al. [220] tested B3LYP and six local density functionals to reproduce 64 high-level W1 energies of reaction for reactions of H_3O^+ and OH^- with microhydration up to $H_{13}O_6^+ + H_9O_5^- \rightarrow 11H_2O$. They found M06-L to be the most accurate DFA tested. In subsequent work, Dahlke et al. [221] assessed eleven DFAs (4 local and 7 nonlocal) against CCSD(T) calculations of the relative energies of six isomers of neutral $(H_2O)_6$. Only the M06-L, M05-2X, and M06-2X DFAs were able to correctly predict the energetic ordering of the isomers.

Leverentz and Truhlar [222] tested eight density functionals for prediction of the geometry and binding energy of a challenging system – the dimer of H_2S and benzene. They concluded that M06-L, M06-2X, and M06 should be useful for a variety of problems in biochemistry and materials where aromatic functional groups can serve as hydrogen bond acceptors. (Prakash et al. [223] had earlier applied the M05-2X functional to study clusters

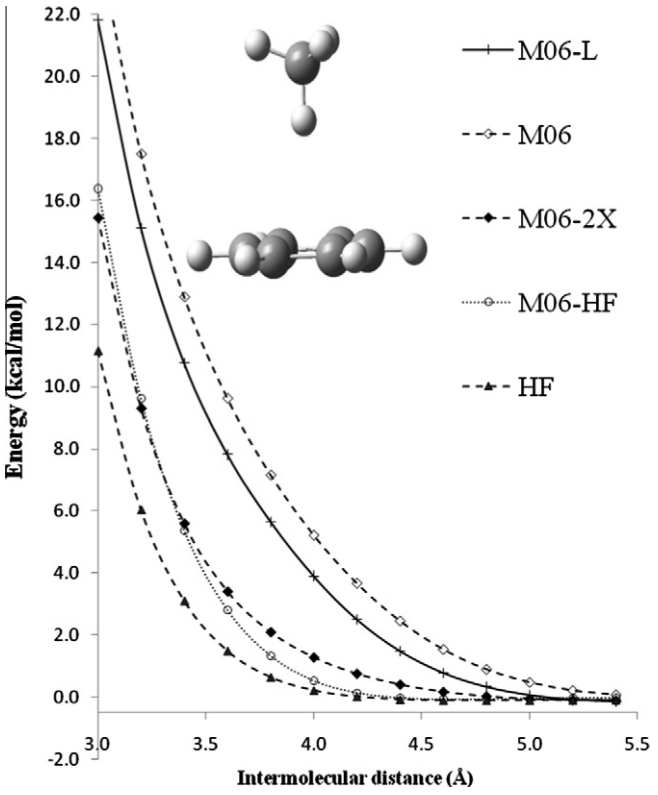

Figure 2. Exchange-only binding energy curves for the C_6H_6–CH_4 complex with the 6-311+G(2df, 2p) basis set. The intermolecular distance is defined as the distance from the carbon atom in CH_4 to the C_6H_6 plane.

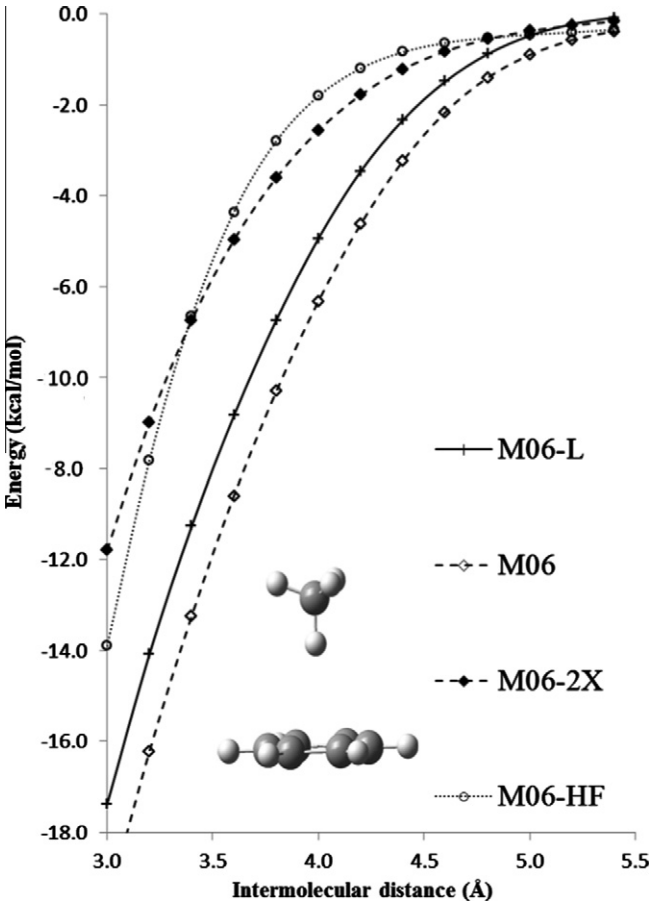

Figure 3. Correlation contribution to binding energy curves for the C_6H_6–CH_4 complex with the 6-311+G(2df, 2p) basis.

of H_2O and benzene.) Bretherick and van Mourik [224] examined the complex of ethyne with methyl isocyanide and the conformations of thioanisole, both of which had earlier shown difference between DFT and WFT. In both cases M05-2X was in good agreement with the best WFT results, although M06-L was found to be inaccurate in the second case.

van Mourik [225] tested a range of DFT methods for their ability to describe the three minima along the Gly rotational profile of one particular Tyr–Gly conformer, and she found that only 'M06-2X and mPW2-PLYP-D predicted the corrected order of stability of the three minima.'

Hohenstein et al. [226] tested the performance of M05-2X and M06-2X for the JSCH-2005 database of noncovalent interaction energies of biological importance. Their assessment shows that PBE-D provides more accurate interaction energies on average for the JSCH-2005 database when compared to M05-2X or M06-2X, whereas M06-2X performs somewhat better than PBE-D for interactions between stacked base pairs.

Bryantsev et al. [227] assessed the performance of B3LYP, X3LYP, and M06-class functionals for predicting binding energies of neutral and charged water clusters. They found that M06-L and M06 give the most accurate binding energies using very extended basis sets. For more affordable basis sets, the best methods for predicting the binding energies of water clusters are M06-L, B3LYP, and M06. M06 also gives more accurate energies for the neutralization reactions, whereas B3LYP gives more accurate energies for the ion hydration reactions.

Bjornsson and Arnson [228] evaluated density functionals for their ability to predict relative conformational energies of a test set of monosubstituted cyclohexanes and six-membered heterocycles. They showed that popular density functionals like B3LYP are unreliable for predicting accurate conformational energies, whereas density functionals that take into account medium-range dispersion interactions like M06-2X and B2PLYP-D (the latter including such effects by a molecular mechanics dispersion term) result in energy differences close to CCSD(T) results.

Cuypers et al. [229] developed a data set of binding enthalpies for phosphine oxide and phosphate complexes with phenol and thiophenol, and their test results show that M06-2X calculations agree well with or are more accurate than more expensive WFT calculations, with an average deviation from the accurate results of less than 1 kcal/mol^{-1}.

Ferrighi et al. [230] employed M06-L to study a series of alkane dimers from methane to decane. They compared the M06-L results to the available WFT benchmarks as well as to values calculated by DFT with molecular mechanics dispersion terms. Their assessment demonstrated that M06-L provides accurate estimates of noncovalent interactions for several systems at moderate computational cost, and M06-L reproduces the trends obtained by the more expensive wave function methods well and represents a valuable and transferable alternative to empirically adding dispersion to DFT by molecular mechanics.

11. Interlocking and crowded molecules

Mechanically interlocking molecules play central roles in some strategies for molecular switches. Benitez et al. [231] reported experimental structural, optical, and binding properties of mechanically interlocked molecules and complexes, and they concluded that these properties are much more accurately predicted with the M06 family of functionals than with the B3LYP and PBE [10] functionals previously used for such materials simulations. Later Spruell et al. [232] applied the M06-L functional to study a

push-button molecular switch, which is also a mechanically interlocked system.

A cyclophane is a molecule in which aliphatic bridges connect nonadjacent positions on an aromatic ring. Cyclophanes can be synthesized with very short interatomic distances, e.g., with methine hydrogens very close to an aromatic ring. We [44] tested 13 DFAs for internuclear distances in two cyclophanes and found mean unsigned errors of 0.006 Å for M05-2X and M06-2X as compared to, for example, 0.007 Å for PBE0 and 0.026 Å for B3LYP.

12. Geophysics, gold clusters, metal–π interactions, and layered structures

We recently reviewed applications of the Minnesota functionals to topics of importance in geophysics, including aqueous and atmospheric chemistry, metal oxides, silicates and siliceous minerals, zeolites, and mineral nanoparticles [233], and general applications of DFT to metal clusters and nanoparticles are reviewed elsewhere [5]. Here we add a few remarks on gold clusters and layered solids.

Gold clusters are particularly interesting because they remain planar up to a fairly large size as compared to other metal clusters. Our group [234] studied anionic Au_n^- with $n = 11–13$ and found that both M06-L and M06 predict the transition from planar to nonplanar to occur between $n = 11$ and 12, in agreement with experiment, whereas previous work [235] had found that PBE0 predicts planarity up to $n = 15$ (the highest n examined in that study). Other previous work [236] had shown that the transition to nonplanar occurs at too high an n for all functionals studied except the LSDA one, which is generally unsatisfactory for energies. Ferrighi et al. [237] studied not only anionic Au_n^- with $n = 8–13$ but also Au_n^+ with $n = 5–10$, and they found that M06-L is the only functional they examined that predicts the planar-to-nonplanar transition correctly in both cases ($n = 12$ for the anion, $n = 8$ for the cation). They then rationalized the calculations in terms of the dependence of the exchange energy density on the reduced density gradient and the kinetic energy density for electron densities in atoms, in bonding regions of molecules, and in nonbonding regions of molecules.

Shi et al. [238] studied neutral Au_n clusters with $n = 2–5$ with 40 DFAs and found the best results with TPSSh [25] and M06-L.

Shao et al. [239] simulated the photoelectron spectrum of Au_{27}^-, which was found to have a low-symmetry one-atom-core–shell isomer structure. The PBE0 DFA predicts that a tubular isomer is 0.2 eV below this structure, whereas M06-L correctly predicts that the core–shell isomer is lower by 0.75 eV.

Understanding the interaction of metal atoms with π systems is especially important for many application in molecular electronics and spintronics. Tishchenko et al. [240] found good agreement of M06-2X calculations with CASPT2 and CCSD(T) calculations in a recent study of charge transfer and biradical states in the interaction of Ca atoms with ethylene and benzene, and M06-2X was then applied to the interaction of Ca with the extended π system of coronene.

In a study [11] focused on the relative importance of the second order term in the density gradient expansion of the density functional for geometries and energies in low-coordination and high-coordination molecules and solids, we found that M06-L was more accurate than other DFAs for the interlayer spacing in graphite and the S–F bond length in the SF_6 molecule, which has a hexacoordinated sulfur atom. Madsen et al. [241], building on their already mentioned analysis in the gold cluster paper [237], analyzed the performance of the M06-L functional for layered solids, including graphite, hexagonal boron nitride, and molybdenum disulfide. This kind of analysis can lead to further improved functionals in the future.

13. Concluding remarks

The Minnesota functionals have been developed by a combination of new functional forms, constraint satisfaction, and semiempirical fitting of parameters to data that involve the important kinds of electronic structural characteristics for many areas of chemistry and chemical physics. Recent diverse validations and successful applications, some of which are reviewed here, give us confidence that these functionals have broader accuracy than previous popular functionals and open the doors to more reliable simulations of many important problems.

Acknowledgments

This work was supported in part by the National Science Foundation and by the Air Force Office of Scientific Research.

References

[1] W. Kohn, L.J. Sham, Phys. Rev. 140 (1965) 1133.
[2] U. von Barth, L. Hedin, J. Phys. C 5 (1972) 1629.
[3] J.P. Perdew, A. Savin, K. Burke, Phys. Rev. A 51 (1995) 4531.
[4] G.E. Scuseria, V.N. Staroverov, in: C.E. Dykstra, G. Frenking, K.S. Kim, G.E. Scuseria (Eds.), Theory and Application of Computational Chemistry: The First 40 years, Elsevier, Amsterdam, 2005, pp. 669–724.
[5] C.J. Cramer, D.G. Truhlar, Phys. Chem. Chem. Phys. 11 (2009) 10757.
[6] D.C. Langreth, M.J. Mehl, Phys. Rev. B 28 (1983) 1809.
[7] C. Lee, W. Yang, R.G. Parr, Phys. Rev. B 37 (1988) 785.
[8] A.D. Becke, Phys. Rev. A 38 (1988) 3098.
[9] J.P. Perdew, J.A. Chevary, S.H. Vosko, K.A. Jackson, M.R. Pederson, D.J. Singh, Phys. Rev. B 46 (1992) 6671.
[10] J.P. Perdew, K. Burke, M. Ernzerhof, Phys. Rev. Lett. 77 (1996) 3865.
[11] Y. Zhao, D.G. Truhlar, J. Chem. Phys. 128 (2008) 184109.
[12] A.D. Becke, J. Chem. Phys. 104 (1996) 1040.
[13] J. Tao, J.P. Perdew, V.N. Staroverov, G.E. Scuseria, Phys. Rev. Lett. 91 (2003) 146401.
[14] Y. Zhao, D.G. Truhlar, J. Chem. Phys. 125 (2006) 194101.
[15] M. Gruning, O. Gritsenko, E.J. Baerends, J. Phys. Chem. A 108 (2004) 4459.
[16] Y. Zhao, D.G. Truhlar, Acc. Chem. Res. 41 (2008) 157.
[17] A.D. Becke, J. Chem. Phys. 98 (1993) 5648.
[18] Y. Zhao, B.J. Lynch, D.G. Truhlar, J. Phys. Chem. A 108 (2004) 4786.
[19] S. Grimme, J. Chem. Phys. 124 (2006) 34108.
[20] M. Dion, H. Rydberg, E. Schroder, D.C. Langreth, B.I. Lundqvist, Phys. Rev. Lett. 92 (2004) 246401.
[21] F. Furche, Phys. Rev. B 64 (2001) 195120.
[22] P.J. Stephens, F.J. Devlin, C.F. Chabalowski, M.J. Frisch, J. Phys. Chem. 98 (1994) 11623.
[23] S.F. Sousa, P.A. Fernandes, M.J. Ramos, J. Phys. Chem. A 111 (2007) 10439.
[24] A.D. Boese, N.C. Handy, J. Chem. Phys. 116 (2002) 9559.
[25] V.N. Staroverov, G.E. Scuseria, J. Tao, J.P. Perdew, J. Chem. Phys. 119 (2003) 12129.
[26] Y. Zhao, B.J. Lynch, D.G. Truhlar, J. Phys. Chem. A 108 (2004) 2715.
[27] Y. Zhao, D.G. Truhlar, J. Phys. Chem. A 108 (2004) 6908.
[28] A.D. Boese, J.M.L. Martin, J. Chem. Phys. 121 (2004) 3405.
[29] Y. Zhao, N.E. Schultz, D.G. Truhlar, J. Chem. Phys. 123 (2005) 161103.
[30] Y. Zhao, N.E. Schultz, D.G. Truhlar, J. Chem. Theory Comput. 2 (2006) 364.
[31] Y. Zhao, D.G. Truhlar, Theor. Chem. Acc. 120 (2008) 215.
[32] A.D. Becke, Int. J. Quantum Chem. 23 (1983) 1915.
[33] A.D. Becke, J. Chem. Phys. 109 (1998) 2092.
[34] A.D. Becke, J. Chem. Phys. 112 (2000) 4020.
[35] H.L. Schmider, A.D. Becke, THEOCHEM 527 (2000) 51.
[36] B.J. Lynch, P.L. Fast, M. Harris, D.G. Truhlar, J. Phys. Chem. A 104 (2000) 4811.
[37] Y. Zhao, B.J. Lynch, D.G. Truhlar, Phys. Chem. Chem. Phys. 7 (2005) 43.
[38] Y. Zhao, N. González-García, D.G. Truhlar, J. Phys. Chem. A 109 (2005) 2012.
[39] E.E. Dahlke, D.G. Truhlar, J. Phys. Chem. B 109 (2005) 15677.
[40] Y. Zhao, D.G. Truhlar, J. Phys. Chem. A 109 (2005) 5656.
[41] N. Schultz, Y. Zhao, D.G. Truhlar, J. Phys. Chem. A 109 (2005) 11127.
[42] J. Zheng, Y. Zhao, D.G. Truhlar, J. Chem. Theory Comput. 5 (2009) 808.
[43] Y. Zhao, D.G. Truhlar, J. Phys. Chem. A 110 (2006) 13126.
[44] Y. Zhao, D.G. Truhlar, J. Chem. Theory Comput. 4 (2008) 1849.
[45] W. Kohn, Rev. Mod. Phys. 71 (1999) 1253.
[46] C. Huang, E.A. Carter, Phys. Rev. B 81 (2010) 045206.
[47] D.G. Truhlar, J. Comput. Chem. 28 (2007) 73.
[48] S. Grimme, F. Neese, J. Chem. Phys. 127 (2007) 154116.
[49] H. Iikura, T. Tsuneda, T. Yanai, K. Hirao, J. Chem. Phys. 115 (2001) 3540.
[50] T.M. Henderson, A.F. Izmaylov, G.E. Scuseria, A. Savin, J. Chem. Phys. 127 (2007) 221103.
[51] R. Baer, E. Livshits, U. Salzner, Annu. Rev. Phys. Chem. 61 (2010) 85.
[52] J.-D. Chai, M. Head-Gordon, J. Chem. Phys. 128 (2008) 84106.
[53] E. Goll, H.-J. Werner, H. Stoll, Z. Phys. Chem. 224 (2010) 481.

[54] Y. Zhao, D.G. Truhlar, J. Am. Chem. Soc. 129 (2007) 8440.
[55] Y. Zhao, D.G. Truhlar, Phys. Chem. Chem. Phys. 10 (2008) 2813.
[56] Y. Zhao, D.G. Truhlar, J. Phys. Chem. C 112 (2008) 4061.
[57] R.S.K. Kishore et al., J. Am. Chem. Soc. 131 (2009) 11106.
[58] S. Lim, N. Park, Appl. Phys. Lett. 95 (2009) 243110.
[59] T.B. Lee, M.L. McKee, J. Am. Chem. Soc. 130 (2008) 17610.
[60] S. Osuna, J. Morera, M. Cases, K. Morokuma, M. Solá, J. Phys. Chem. A 113 (2009) 9721.
[61] M. Izquierdo, S. Osuna, S. Filippone, A. Martin-Domenech, M. Sola, N. Martin, J. Org. Chem. 74 (2009) 6253.
[62] J. Vura-Weis, M.A. Ratner, M.R. Wasielewski, J. Am. Chem. Soc. 132 (2010) 1738.
[63] R. Peverati, K.K. Baldridge, J. Chem. Theory Comput. 4 (2008) 2030.
[64] M. Prakash, V. Subramanian, S.R. Gadre, J. Phys. Chem. A 113 (2009) 12660.
[65] C.E. Check, T.M. Gilbert, J. Org. Chem. 70 (2005) 9828.
[66] E.I. Izgorodina, M.L. Coote, L. Radom, J. Phys. Chem. A 109 (2005) 7558.
[67] P.R. Carlier, N. Deora, T.D. Crawford, J. Org. Chem. 71 (2006) 1592.
[68] S. Grimme, Angew. Chem. Int. Ed. 45 (2006) 4460.
[69] P.R. Schreiner, A.A. Fokin, R.A. Pascal Jr., A. de Meijere, Org. Lett. 8 (2006) 3635.
[70] M.D. Wodrich, C. Corminboeuf, P.V.R. Schleyer, Org. Lett. 8 (2006) 3631.
[71] E.I. Izgorodina, M.L. Coote, J. Phys. Chem. A 110 (2006) 2486.
[72] E.I. Izgorodina, M.L. Coote, Chem. Phys. 324 (2006) 96.
[73] S. Grimme, M. Steinmetz, M. Korth, J. Chem. Theory Comput. 3 (2007) 42.
[74] S. Grimme, M. Steinmetz, M. Korth, J. Org. Chem. 72 (2007) 2118.
[75] P.R. Schreiner, Angew. Chem. Int. Ed. 46 (2007) 4217.
[76] E.I. Izgorodina, D.R.B. Brittain, J.L. Hodgson, E.H. Krenske, C.Y. Lin, M. Namazian, M.L. Coote, J. Phys. Chem. A 111 (2007) 10754.
[77] Y. Zhao, D.G. Truhlar, Org. Lett. 8 (2006) 5753.
[78] M.D. Wodrich, C. Corminboeuf, P.R. Schreiner, A.A. Fokin, P.V.R. Schleyer, Org. Lett. 9 (2007) 1851.
[79] T.A. Rokob, A. Hamza, I. Papai, Org. Lett. 9 (2007) 4279.
[80] Y. Zhao, D.G. Truhlar, J. Org. Chem. 72 (2007) 295.
[81] Y. Zhao, D.G. Truhlar, J. Phys. Chem. A 112 (2008) 1095.
[82] S.N. Steinmann, M.D. Wodrich, C. Corminboeuf, Theor. Chem. Acc., in press. doi:10.1007/s00214-010-0818-3.
[83] A.N. Garr, D.H. Luo, N. Brown, C.J. Cramer, K.R. Buszek, D. VanderVelde, Org. Lett. 12 (2010) 96.
[84] D. Sadowsky, K. McNeill, C.J. Cramer, Faraday Discuss. 145 (2010) 507.
[85] M. Aginagalde, Y. Vara, A. Arrieta, R. Zangi, V.L. Cebolla, A. Delgado-Camón, F.P. Cossío, J. Org. Chem. 75 (2010) 2776.
[86] X. Bao, S. Rieth, S. Stojanovic, C.M. Hadad, J.D. Badjic, Angew. Chem. Int. Ed. 49 (2010) 4816.
[87] O. Bertran, J. Torras, C. Aleman, J. Phys. Chem. C 114 (2010) 11074.
[88] S.O. Wallevik et al., J. Phys. Chem. A 114 (2010) 2127.
[89] W.-G. Liu, S.V. Zybin, S. Dasgupta, T.M. Klapoltke, W.A. Goddard III, J. Am. Chem. Soc. 131 (2009) 7490.
[90] I.Y. Zhang, J. Wu, X. Xu, Chem. Commun. 46 (2010) 3057.
[91] R. Li, Y. Zhao, D.G. Truhlar, Chem. Comm., in press.
[92] M.M. Meyer, S.R. Kass, J. Org. Chem. 75 (2010) 4274.
[93] A. Beste, A.C. Buchanan III, J. Org. Chem. 74 (2009) 2837.
[94] A. Beste, A.C. Buchanan III, Energy Fuels 24 (2010) 2857.
[95] Y. Zhao, D.G. Truhlar, J. Chem. Theory Comput. 6 (2010) 1104.
[96] K.W. Wiitala, Z. Tian, C.J. Cramer, T.R. Hoye, J. Org. Chem. 73 (2008) 3024.
[97] (a) S. Rayne, K. Forest, J. Mol. Struct. THEOCHEM 948 (2010) 102; (b) R.A. Powoski, G.S. Grubbs II, J.o.M.S.S.A. Cooke, J. Mol. Struct. 963 (2010) 106.
[98] D. Jacquemin, V. Wathelet, E.A. Perpete, C. Adamo, J. Chem. Theory Comput. 5 (2009) 2420.
[99] D. Jacquemin, E.A. Perpète, I. Ciofini, C. Adamo, R. Valero, Y. Zhao, D.G. Truhlar, J. Chem. Theory Comput. 6 (2010) 2071.
[100] C. Adamo, V. Barone, J. Chem. Phys. 110 (1999) 6158.
[101] M. Ernzerhof, G.E. Scuseria, J. Chem. Phys. 110 (1999) 5029.
[102] H.L. Schmider, A.D. Becke, J. Chem. Phys. 108 (1998) 9624.
[103] A. Dreuw, M. Head-Gordon, J. Chem. Phys. 119 (2003) 2943.
[104] M. Parac, S. Grimme, Chem. Phys. Chem. 4 (2003) 292.
[105] R. Li, J. Zheng, D.G. Truhlar, Phys. Chem. Chem. Phys. 12 (2010) 12697.
[106] T. Yanai, D.P. Tew, N.C. Handy, Chem. Phys. Lett. 393 (2004) 51.
[107] A.V. Marenich, C.J. Cramer, D.G. Truhlar, J. Chem. Theory Comput. 6 (2010) 2829.
[108] M. Caricato, B. Mennucci, J. Tomasi, F. Ingrosso, R. Camoni, S. Corni, G. Scalmani, J. Chem. Phys. 124 (2006) 124520.
[109] F. Santoro, V. Barone, R. Improta, J. Comp. Chem. 29 (2008) 957.
[110] A.J.A. Aquino, D. Nachtigallova, P. Hobza, D.G. Truhlar, C. Hättig, H. Lischka, J. Comput. Chem., in press.
[111] R. Cammi, S. Corni, B. Mennucci, J. Tomasi, J. Chem. Phys. 122 (2005) 10451.
[112] K. Swiderek, P. Paneth, J. Phys. Org. Chem. 22 (2009) 845.
[113] K. Edgecombe, A.D. Becke, Chem. Phys. Lett. 244 (1995) 427.
[114] P.D. Patel, A.E. Masunov, J. Phys. Chem. A 113 (2009) 8409.
[115] P.D. Patel, A.E. Masunov, Lect. Notes Comput. Sci. 5545 (2009) 211.
[116] Y. Zhao, D.G. Truhlar, J. Phys. Chem. A 110 (2006) 10478.
[117] J. Kim, S. Jun, J. Kim, J.P.C.A.H. Ihee, J. Phys. Chem. A 113 (2009) 11059.
[118] I.M. Alecu, J. Zheng, Y. Zhao, D.G. Truhlar, J. Chem. Theory Comput. 6 (2010) 2872.
[119] C.A. Jimenez-Hoyos, B.G. Janesko, G.E. Scuseria, Phys. Chem. Chem. Phys. 10 (2008) 6621.
[120] M.M. Meyer, S.R. Kass, J. Phys. Chem. A 114 (2010) 4086.
[121] J.P. Plumley, J.D. Evanseck, J. Chem. Theory Comput. 4 (2008) 1249.
[122] B.G. Janesko, J. Chem. Theory Comput. 6 (2010) 1825.
[123] R.P. Dias, J. Mauro S. L. Prates, W.B.D. Almeida, W.R. Rocha, Int. J. Quant. Chem., in press. doi:10.1002/qua.22 590.
[124] J.P. Austin, N.A. Burton, I.H. Hillie, M. Sundararajan, M.A. Vincent, Phys. Chem. Chem. Phys. 11 (2009) 1143.
[125] M. Oncák, D. Schröder, P. Slavicek, J. Comput. Chem. 31 (2010) 2294.
[126] Y. Zhao, D.G. Truhlar, J. Phys. Chem. C 112 (2008) 6860.
[127] T. Maihom, B. Boekfa, J. Sirijaraensre, T. Nanok, M. Probst, J. Limtrakul, J. Phys. Chem. C 113 (2009) 6654.
[128] J.M. Vollmer, E.V. Stefanovich, T.N. Truong, J. Phys. Chem. B 103 (1999) 9415.
[129] B. Boekfa, S. Choomwattana, P. Khongpracha, J. Limtrakul, Langmuir 25 (2009) 12990.
[130] C. Kumsapaya, K. Bobuatong, P. Khongpracha, Y. Tantirungrotechai, J. Limtrakul, J. Phys. Chem. C 113 (2009) 16128.
[131] T. Maihom, P. Pantu, C. Tachakritikul, M. Probst, J. Limtrakul, J. Phys. Chem. C 114 (2010) 7850.
[132] F. Labat, A.H. Fuchs, C. Adamo, J. Phys. Chem. Lett. 1 (2010) 763.
[133] S. Grimme, J. Comput. Chem. 27 (2006) 1787.
[134] K. Yang, J. Zheng, Y. Zhao, D.G. Truhlar, J. Chem. Phys. 132 (2010) 164117.
[135] B. Hammer, L.B. Hansen, J.K. Nørskov, Phys. Rev. B 59 (1999) 7413.
[136] Y. Zhang, W. Yang, Phys. Rev. Lett. 80 (1998) 890.
[137] A.C. Tsipis, A.G. Orpen, J.N. Harvey, Dalton Trans. (2005) 2849.
[138] M.S. Sanford, J.A. Love, R.H. Grubbs, J. Am. Chem. Soc. 123 (2001) 6543.
[139] C. Adlhart, P. Chen, Helv. Chim. Acta 86 (2003) 941.
[140] Y. Zhao, D.G. Truhlar, Org. Lett. 9 (2007) 1967.
[141] S. Torker, D. Merki, P. Chen, J. Am. Chem. Soc. 130 (2008) 4808.
[142] Y. Zhao, D.G. Truhlar, J. Chem. Theory Comput. 5 (2008) 324.
[143] P. Sliwa, J. Handzlik, Chem. Phys. Lett. 493 (2010) 273.
[144] S. Pandian et al., Chem. Phys. Lett. 476 (2009) 37.
[145] D. Benitez, E. Tkatchouk, W.A. Goddard, Chem. Commun. (2008) 6194.
[146] D. Benitez, E. Tkatchouk, W.A. Goddard, Organometallics 28 (2009) 2643.
[147] I.C. Stewart, D. Benitez, D.J. O'Leary, E. Tkatchouk, M.W. Day, W.A. Goddard, R.H. Grubbs, J. Am. Chem. Soc. 131 (2009) 1931.
[148] N. Sieffert, M. Bühl, Inorg. Chem. 48 (2009) 4622.
[149] J.P. Perdew, Phys. Rev. B 33 (1986) 8822.
[150] N. Sieffert, M. Bühl, J. Am. Chem. Soc. 132 (2010) 8056.
[151] Y. Minenkov, G. Occhipinti, V.R. Jensen, J. Phys. Chem. A 113 (2009) 11833.
[152] F. Huang, G. Lu, L. Zhao, H. Li, Z.-X. Wang, J. Am. Chem. Soc. 132 (2010) 12388.
[153] F. Bozoglian et al., J. Am. Chem. Soc. 131 (2009) 15176.
[154] A. Fedorov, M.-E. Moret, P. Chen, J. Am. Chem. Soc. 130 (2008) 8880.
[155] A. Fedorov, L. Batiste, E.P.A. Couzijn, P. Chen, ChemPhysChem 11 (2010) 1002.
[156] D. Benitez, N.D. Shapiro, E. Tkatchouk, Y.M. Wang, W.A. Goddard, F.D. Toste, Nat. Chem. 1 (2009) 482.
[157] D. Benitez, E. Tkatchouk, A.Z. Gonzalez, W.A. Goddard, F.D. Toste, Org. Lett. 11 (2009) 4798.
[158] J. Nyhlén, T. Privalov, J. Mol. Cat. A 324 (2010) 97.
[159] R.F. Heck, J.P. Nolley Jr., J. Org. Chem. 37 (1972) 2320.
[160] D. Milstein, J.K. Stille, J. Am. Chem. Soc. 100 (1978) 3636.
[161] A.O. King, E.-I. Negishi, F.J. Villani Jr., A. Silveira Jr., J. Org. Chem. 43 (1978) 358.
[162] N. Miyaura, A. Suzuki, Chem. Rev. 95 (1995) 2457.
[163] A. Ikeda, Y. Nakao, H. Sato, S. Sakaki, J. Phys. Chem. A 111 (2007) 7124.
[164] B.B. Averkiev, Y. Zhao, D.G. Truhlar, J. Mol. Cat. A 324 (2010) 80.
[165] A. Karton, D. Grozman, J.M.L. Martin, J. Phys. Chem. A 113 (2009) 8434.
[166] J.-D. Chai, M. Head-Gordon, Phys. Chem. Chem. Phys. 10 (2008) 6615.
[167] S.T. Mutter, J.A. Platts, Chem. Eur. J. 16 (2010) 5391.
[168] A.D. Becke, J. Chem. Phys. 98 (1993) 1372.
[169] Y.-W. Huang, S.-L. Lee, Chem. Phys. Lett. 492 (2010) 98.
[170] E.P.A. Couzijn, E. Zocher, A. Bach, P. Chen, Chem. Eur. J. 16 (2010) 5408.
[171] C. Metallinos, J. Zaifman, T. Dudding, L.V. Belle, K. Taban, Adv. Synth. Catal. 352 (2010) 1967.
[172] B. Dutta, B.F.E. Curchod, P. Campomanes, E. Solari, R. Scopelliti, U. Röthlisberger, K. Severin, Chem. Eur. J. 16 (2010) 8400.
[173] E. Ruiz, Chem. Phys. Lett. 460 (2008) 336.
[174] R. Valero, R. Costa, I.d.P.R. Moreira, D.G. Truhlar, F. Illas, J. Chem. Phys. 128 (2008) 114103.
[175] J. Zheng, Y. Zhao, D.G. Truhlar, J. Chem. Theory Comput. 3 (2007) 569.
[176] A. Gonzàlez-Lafont, T.N. Truong, D.G. Truhlar, J. Phys. Chem. 95 (1991) 4618.
[177] Y.-P. Liu, G.C. Lynch, T.N. Truong, D.-h. Lu, D.G. Truhlar, B.C. Garrett, J. Am. Chem. Soc. 115 (1993) 2408.
[178] Y.-P. Lu, D.-h. Lu, A. Gonzàlez-Lafont, D.G. Truhlar, B.C. Garrett, J. Am. Chem. Soc. 115 (1993) 7806.
[179] J. Pu, D.G. Truhlar, J. Chem. Phys. 116 (2002) 1468.
[180] Y. Kim, J.R. Mohrig, D.G. Truhlar, J. Am. Chem. Soc. 132 (2010) 11071.
[181] A.V. Marenich, R.M. Olson, C.P. Kelly, C.J. Cramer, D.G. Truhlar, J. Chem. Theory Comput. 3 (2007) 2011.
[182] B.A. Ellingson, D.G. Truhlar, J. Am. Chem. Soc. 129 (2007) 12765.
[183] T. Hayama, K.K. Baldridge, Y.-T. Wu, A. Linden, J.S. Siegel, J. Am. Chem. Soc. 130 (2008) 1583.
[184] J.J. Zheng, S.X. Zhang, D.G. Truhlar, J. Phys. Chem. A 112 (2008) 11509.
[185] J. Zheng, D.G. Truhlar, J. Phys. Chem. A 113 (2009) 11919.
[186] J. Zheng, D.G. Truhlar, Phys. Chem. Chem. Phys. 12 (2010) 7782.
[187] A. Pabis, P. Paluch, J. Szala, P. Paneth, J. Chem. Theory Comput. 5 (2009) 33.
[188] Y. Kim et al., J. Chem. Theory Comput. 5 (2009) 59.

[189] Y. Kim, C.J. Cramer, D.G. Truhlar, J. Phys. Chem. A 113 (2009) 9109.
[190] X. Chen, C.K. Regan, S.L. Craig, E.H. Krenske, K.N. Houk, W.L. Jorgensen, J.I. Brauman, J. Am. Chem. Soc. 131 (2009) 16162.
[191] J. Gao, D.G. Truhlar, Annu. Rev. Phys. Chem. 53 (2002) 467.
[192] J. Gao, S. Ma, D.T. Major, K. Nam, J. Pu, D.G. Truhlar, Chem. Rev. 106 (2006) 3188.
[193] C.H. Suresh, N. Mohan, K.P. Vijayalakshmi, R. George, J.M. Mathew, J. Comput. Chem. 30 (2008) 1392.
[194] H. Valdes, K. Pluhackova, M.L. Pitonak, J. Rezac, P. Hobza, Phys. Chem. Chem. Phys. 10 (2008) 2747.
[195] P. Jurecka, J. Cerny, P. Hobza, D.R. Salahub, J. Comput. Chem. 28 (2007) 555.
[196] J. Gu, J. Wang, J. Leszczynski, Y. Xie, H.F. Schaefer III, Chem. Phys. Lett. 459 (2008) 164.
[197] A. Darwanto, J.A. Theruvathu, J.L. Sowers, D.K. Rogstad, T. Pascal, W.A. Goddard, L.C. Sowers, J. Biol. Chem. 284 (2009) 15835.
[198] R.L. Wood, B.J. Young-Dixon, A. Roy, B.C. Gay, R.L. Johnson, E.A. Amin, THEOCHEM 944 (2010) 76.
[199] C. Adamo, V. Barone, J. Chem. Phys. 108 (1998) 664.
[200] P.J. Wilson, T.J. Bradley, D.J. Tozer, J. Chem. Phys. 115 (2001) 9233.
[201] K.G. Byler, C. Wang, W.N. Setzer, J. Mol. Modeling 15 (2009) 1417.
[202] A. Ebrahimi, M. Habibi-Khorassani, A.R. Gholipour, H.R. Masoodi, Theor. Chem. Acc. 124 (2009) 115.
[203] J. Cao, T. van Mourik, Chem. Phys. Lett. 485 (2010) 40.
[204] D. Toroz, T. van Mourik, Phys. Chem. Chem. Phys. 12 (2010) 3463.
[205] T. van Mourik, V.I. Danilov, V.V. Dailidonis, N. Kurita, H. Wakabayashi, T. Tsukamoto, Theor. Chem. Acc. 125 (2010) 233.
[206] J.C. Hargis, H.F. Schaefer, K.N. Houk, S.E. Wheeler, J. Phys. Chem. A 114 (2010) 2038.
[207] J. Ortega-Castro, M. Adrover, J. Frau, A. Salv, J. Donoso, F. Munoz, J. Phys. Chem. A 114 (2010) 4634.
[208] L.R. Rutledge, S.D. Wetmore, Can. J. Chem. 88 (2010) 815.
[209] Y.K. Kang, B.J. Byun, J. Comput. Chem. 31 (2010) 2915.
[210] A. Marenich, C.J. Cramer, D.G. Truhlar, J. Phys. Chem. B 113 (2009) 6378.
[211] Y.K. Kang, B.J. Byun, H.S. Park, Biopolymer in press. doi:10.1002/bip.21 534.
[212] J.R. Greenwood, D. Calkins, A.P. Sullivan, J.C. Shelley, J. Comput. Aided Mol. Design 24 (2010) 591.
[213] J. Kona, I. Tvaroska, Chem. Papers 63 (2009) 598.
[214] Y. Zhao, D.G. Truhlar, J. Chem. Theory Comput. 1 (2005) 415.
[215] Y. Zhao, D.G. Truhlar, J. Phys. Chem. A 110 (2006) 5121.
[216] Y. Zhao, D.G. Truhlar, J. Chem. Theory Comput. 2 (2006) 1009.
[217] Y. Zhao, D.G. Truhlar, J. Chem. Theory Comput. 3 (2007) 289.
[218] J. Cerny, P. Hobza, Phys. Chem. Chem. Phys. 9 (2007) 5291.
[219] K.E. Riley, J. Vondrasek, P. Hobza, Phys. Chem. Chem. Phys. 9 (2007) 5555.
[220] E.E. Dahlke, M.A. Orthmeyer, D.G. Truhlar, J. Phys. Chem. A 112 (2008) 2372.
[221] E.E. Dahlke, R.M. Olson, H.R. Leverentz, D.G. Truhlar, J. Phys. Chem. A 112 (2008) 3976.
[222] H.R. Leverentz, D.G. Truhlar, J. Phys. Chem. A 112 (2008) 6009.
[223] M. Prakash, K.G. Samy, V. Subramanian, J. Phys. Chem. A 113 (2009) 13845.
[224] N.H. Bretherik, T. van Mourik, J. Chem. Theory Comput. 6 (2010) 2687.
[225] T. van Mourik, J. Chem. Theory Comput. 4 (2008) 1610.
[226] E.G. Hohenstein, S.T. Chill, D. Sherrill, J. Chem. Theory Comput. 4 (2008) 1996.
[227] V.S. Bryantsev, M.S. Diallo, A.C.T. van Duin, W.A. Goddard III, J. Chem. Theory Comput. 5 (2009) 1016.
[228] R. Bjornsson, I. Arnason, Phys. Chem. Chem. Phys. 11 (2009) 8689.
[229] R. Cuypers, E.J.R. Sudhölter, H. Zuilhof, ChemPhysChem 11 (2010) 2230.
[230] L. Ferrighi, G.K.H. Madsen, B. Hammer, Chem. Phys. Lett. 492 (2010) 183.
[231] D. Benitez, E. Tkatchouk, I. Yoon, J.F. Stoddart, W.A. Goddard, J. Am. Chem. Soc. 130 (2008) 14928.
[232] J.M. Spruell et al., J. Am. Chem. Soc. 131 (2009) 11571.
[233] Y. Zhao, D.G. Truhlar, Rev. Mineral. Geochem. 71 (2010) 19.
[234] M. Mantina, R. Valero, D.G. Truhlar, J. Chem. Phys. 131 (2009) 064706.
[235] F. Furche, R. Ahlrichs, P. Weis, C. Jacob, S. Gilb, T. Bierweiler, M. Kappes, J. Chem. Phys. 117 (2002) 6982.
[236] M.P. Johansson, A. Lechtken, D. Schoos, M. Kappes, P. Furche, Phys. Rev. A 77 (2008) 053202.
[237] L. Ferrighi, B. Hammer, G.K.H. Madsen, J. Am. Chem. Soc. 131 (2009) 10605.
[238] Y.-K. Shi, Z.H. Li, K.-N. Fan, J. Phys. Chem. A. 114 (2010) 10297.
[239] N. Shao, W. Huang, Y. Gao, L.-M. Wang, X. Li, L.-S. Wang, X.C. Zeng, J. Am. Chem. Soc. 132 (2010) 6596.
[240] O. Tishchenko, R. Li, D.G. Truhlar, Proc. Natl. Acad. Sci. USA, 45 (2010) 19139.
[241] G.K.H. Madsen, L. Ferrighi, B. Hammer, J. Phys. Chem. Lett. 1 (2010) 515.
[242] K. Shibasaki, F. Fujii, N. Mikami, S. Tsuzuki, J. Phys. Chem. A 110 (2006) 4397.

Yan Zhao received a B.S. from Fudan University in 1993, and a M.E. from Sichuan University in 1996. In 2005, he received a Ph.D. in Chemistry from the University of Minnesota, where his advisor was Donald Truhlar. He also did 3 years of postdoctoral research in Truhlar's group. His research in Truhlar's group focused on development and application of new generation of density functionals with broad accuracy for chemistry. He joined HP in 2009 as a molecular modeling scientist, and his research at HP focuses on employing state-of-the-art multiscale modeling techniques to tackle challenging problems in printing materials.

Don Truhlar is Regents Professor of Chemistry, Chemical Physics, Nanoparticle Science and Engineering, and Scientific Computation in the Department of Chemistry at the University of Minnesota, where he has served on faculty since 1969. He was bon in Chicago, received a B.A. from St. Mary's College of Minnesota, and a Ph.D. from Caltech where his adviser was Aron Kuppermann. His research areas are quantum mechanical chemical dynamics, electronic structure theory, and statistical mechanics. His research is funded by the NSF, DOE, NIH, AFOSR, and ARO. He is a Fellow of the AAAS, ACS, APS, RSC, and WATOC and a member of the IAQMS and the National Academy of Sciences (USA). He is recipient of ACS Award in Computers in Chemical and Pharmaceutical Research, Minnesota Award, NAS Award for Scientific Reviewing, ACS Debye Award for Physical Chemistry, Lise Meitner Lectureship Award, Schrödinger Medal of WATOC, Herschbach Award for Molecular Collision Dynamics, and Doctor honoris causa of Technical University of Lodz. He owes his happiness and success to his wife Jane, his daughters Sara and Stephanie, and his staggeringly talented students and colleagues.